Author(s): Provatas, N. & Ala-Nissilä, Tapio & Alava, M. J.

Title: Growth and Structure of Random Fibre Clusters and Cluster Networks

Year: 1995

Version: Final published version

Please cite the original version:

Provatas, N. & Ala-Nissilä, Tapio & Alava, M. J. 1995. Growth and Structure of Random Fibre Clusters and Cluster Networks. Physical Review Letters. Volume 75, Issue 19. P. 3556-3559. ISSN 0031-9007 (printed). DOI: 10.1103/physrevlett.75.3556.

Growth and Structure of Random Fibre Clusters and Cluster Networks

N. Provatas,[1] T. Ala-Nissila,[1,3] and M. J. Alava[2]

[1]*University of Helsinki, Research Institute for Theoretical Physics, P.O. Box 9, FIN-00014 Helsinki, Finland*

[2]*Laboratory of Physics, Helsinki University of Technology, Otakaari 1M, FIN-02150 Espoo, Finland*

[3]*Brown University, Department of Physics, Box 1843, Providence, Rhode Island 02912*

and Tampere University of Technology, Department of Physics, P.O. Box 692, FIN-33101 Tampere, Finland

(Received 29 June 1995)

We study the properties of 2D fibre clusters and networks formed by deposition processes. We first examine the growth and scaling properties of single clusters. We then consider a network of such clusters, whose spatial distribution obeys some effective pair distribution function. In particular, we derive an expression for the two-point density autocorrelation function of the network, which includes the internal structure of a cluster and the effective cluster-cluster pair distribution function. This formula can be applied to obtain information about nontrivial correlations in fibre networks.

PACS numbers: 81.15.Lm, 61.43.Hv, 81.35.+k, 82.70.Kj

There are many phenomena in nature that can be viewed as deposition problems, brought about through various transport mechanisms that bring particles to a surface. They include a multitude of processes such as deposition of colloidal, polymer, and fibre particles [1–7]. Many deposition phenomena involve particles whose size is large compared to their mutual interaction range, and so the main deposition mechanism is due to particle exclusion. Among the most studied in this class is the random sequential adsorption model [1,2]. There particles are deposited on a surface and either stick or are rejected according to certain exclusion rules, with a maximum coverage (the "jamming limit") less than unity. This is in contrast to multilayer growth [1,6,7].

Processes of particle deposition may often begin from colloidal suspensions, solid particles suspended in a fluid. For some such systems, the interparticle repulsion is strong enough to prevent multilayer growth [3]. However, the existence of dispersion forces can cause the particles to flocculate, or aggregate, and to precipitate out of the suspension [7,8]. For larger particles or clusters of particles, gravity often induces sedimentation out of the suspension [9].

A particularly interesting class of deposition-related problems that has received little attention is the deposition of fibres, fibre clusters, and the formation of fibre networks. Perhaps the most practical application of fibre deposition is that of paper making. During its formation paper undergoes several stages, beginning as a colloidal suspension of fibres and ending up as a deposition of fibres on a surface, when the fluid is drained out. There have been many attempts to model the structure of fibre networks [4,5,10–12]. Much of this work has focused on the calculation of power spectra of ideal random fibre networks and their subsequent comparison with mass distribution data obtained from paper-making experiments.

In some sedimentation problems, such as in the making of laboratory paper sheets, the fibres can flocculate while still in solution [13]. This may occur for a variety of reasons, ranging from mechanical fibre-fibre interactions to hydrodynamic forces in the suspension [9]. In such circumstances the resulting network may consist of clusters of fibres. Similar clusters are also expected to occur in other deposition problems. This is one of the main motivations for our work where we present a detailed study of the statistical properties of deposition processes involving individual fibres and clusters.

We start with a simple model of deposition of fibres of length λ and width ω on a 2D plane. Deposition begins from an initial seed fibre. At each deposition event only a fibre that overlaps at least one fibre already in the cluster is kept. This growth rule is motivated by the adhesive sticking of fibres. The process forms a connected cluster of N fibres that is statistically spherically symmetric. Thus it is possible to define an average maximum radius $R(N)$. Figure 1 shows one configuration of a computer

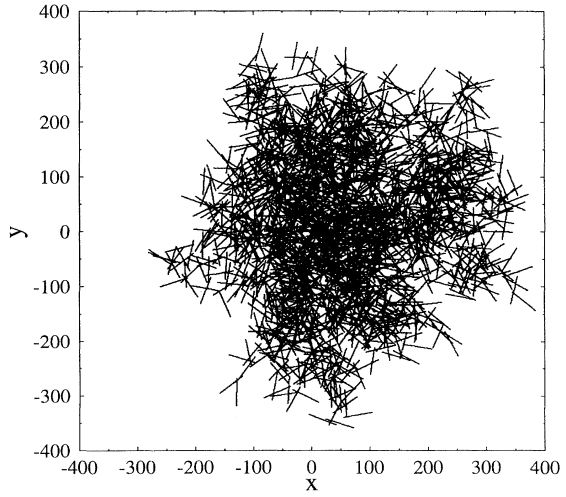

FIG. 1. A fibre cluster made of 2000 fibres of dimension $\lambda \times \omega = 50 \times 1$. The cluster is constructed by depositing fibres randomly, keeping only those that form one connected fibre cluster, beginning from an initial fibre.

 0031-9007/95/75(19)/3556(4)$06.00

generated N cluster on a lattice, where $N = 2000$. We find that for $N \gg 1$ the radius satisfies

$$R(N) = BN^{\beta}, \tag{1}$$

where the exponent $\beta \approx 1/3$, over the range of N examined and for all fibre geometries simulated, while the constant B depends only on fibre dimensions. Figure 2 shows a plot of $R(N)$ for two different types of fibre geometries; $\lambda \times \omega = 20 \times 1$ and $\lambda \times \omega = 50 \times 1$ showing the corresponding plots on a log-log scale. We note that Eq. (1) also gives the number of fibres in a cluster directly from the radius.

The exponent $1/3$ in Eq. (1) also arises from the following simple argument. Assume we have a cluster of average radius $R(N)$ composed of N fibres of linear dimension $a = \sqrt{\lambda\omega}$. Next if we deposit an additional ΔN fibres onto the cluster its radius grows by ΔR and area by ΔA. The change in the cluster area $\Delta A = \frac{1}{2}a^2\Delta N(2\pi Ra)/(\pi R^2) = 2\pi R\Delta R$, which in the continuum limit gives Eq. (1), with $B = (3/2\pi)^{1/3}a$. The factor $2\pi Ra/\pi R^2$ comes from the "active" zone at the edge of the cluster, which is the only region where added fibres increase the area.

Another measure to characterize the N cluster is the radial mass probability per unit area. This quantity is given by

$$\rho_N(r) = \frac{m_N(r)}{\int_0^{\infty} m_N(r)\, dr}, \tag{2}$$

where $m_N(r)$ represents the mass per unit area at a radial distance r from the center of the cluster. For large N, the normalized average mass probability density $P_N(r) \equiv \langle \rho_N(r) \rangle$ can be written as

$$P_N(r) = \frac{1}{\gamma R(N)} f(r/R(N)), \tag{3}$$

where $\gamma = \int_0^{\infty} uf(u)\, du$ and where the average implies an ensemble average over all N cluster configurations. Figure 3 shows a plot of $P_N(r)$ for five different values of N while the scaling function $f(r)$ is shown in the inset. The scaling function f is universal for the values of λ and ω studied here. The mass probability distributions have a peaklike component at the origin, continuing almost linearly for the greater part of their width.

At the edge of the cluster, there is a fast decaying region that also scales as shown in Fig. 3. This is associated with the rough edge of the cluster, which we can examine in the context of kinetic roughening of growing interfaces [14]. Defining fluctuations of the radius as $W(N) = \langle [\tilde{R}(N) - R(N)]^2 \rangle^{1/2}$, where $\tilde{R}(N)$ is the radius for one cluster, we find it to grow as $W \sim N^x$, where x is consistent with $1/3$ as expected since $W/R = \text{const}$. The roughness of the cluster is expected to alter the percolation threshold of a random fibre-cluster network from that of a distribution of solid disks [15].

We now consider a *disordered fibre network* constructed by deposition of N clusters. This model is completely general and the only assumption is that there exists an effective spatial pair distribution function between any two clusters. One plausible application of such a network is the description of sedimentation of fibre suspensions containing flocs of fibres, as discussed above.

Starting from a distribution of n_c fibre clusters, labeled by an index i, and where the ith cluster contains $N(i)$ fibres, the mass distribution of the resulting network is $M(\vec{x}) = \sum_{i=1}^{n_c} m_{N(i)}(\vec{x} - \vec{x}_i)$, where $m_{N(i)}$ is the mass density and $\vec{x}_i$ the coordinate of the center of the ith cluster. The two-point density autocorrelation function of

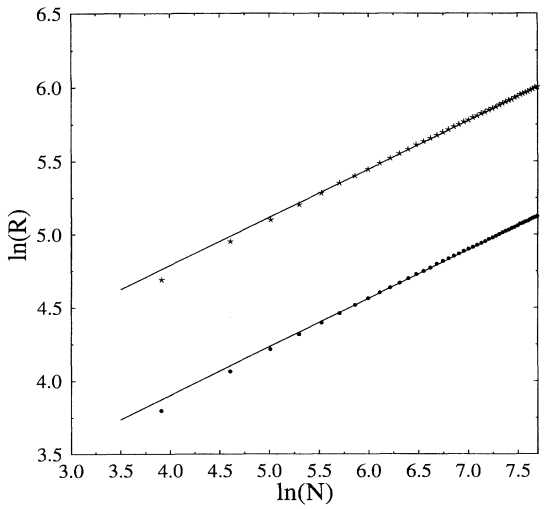

FIG. 2. A plot of $R(N)$ on a log-log scale. In the bottom curve $\lambda \times \omega = 20 \times 1$, while for the top curve $\lambda \times \omega = 50 \times 1$. The solid lines are drawn for comparison and have a slope of $1/3$.

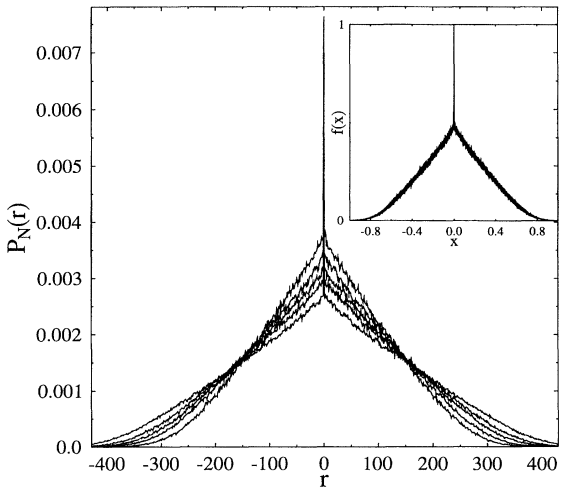

FIG. 3. The radial mass probability per unit area, for $N = 1500$, 2000, 2500, 3000, and 4000 fibres, with $\lambda \times \omega = 50 \times 1$. The inset shows the scaling function $f(x)$ vs $x = r/R$.

this network is given by [10]

$$G(\vec{r}) = \lim_{A\to\infty} F^{-1}\left(\frac{\langle|\hat{M}(\vec{k})|^2\rangle}{A}\right), \quad (4)$$

where A is the area over which the 2D network is deposited, F^{-1} is the inverse Fourier transform, and the average is taken over all network configurations. The Fourier transform of $M(\vec{x})$ is given by

$$|\hat{M}(\vec{k})|^2 = \sum_{n=1}^{n_c}\sum_{m=1}^{n_c} e^{-2\pi i\vec{k}\cdot(\vec{x}_n-\vec{x}_m)} I_{N(n)} I^*_{N(m)}, \quad (5)$$

where $I_{N(n)}$ is the Fourier transform of $m_{N(n)}(\vec{x})$ evaluated over the area of the $N(n)$ cluster. The coordinate in $I_{N(n)}$ is defined relative to the center of the nth cluster. Taking the ensemble average of Eq. (5) we make the assumption that the description of individual clusters is independent of the positions of their centers. Thus

$$\langle e^{-2\pi i\vec{k}\cdot(\vec{x}_n-\vec{x}_m)} I_{N(n)} I^*_{N(m)}\rangle = \langle e^{-2\pi i\vec{k}\cdot(\vec{x}_n-\vec{x}_m)}\rangle \times \langle I_{N(n)} I^*_{N(m)}\rangle. \quad (6)$$

Next, making the assumption that the internal structure of any given cluster is independent of the others, we write $\langle I_{N(n)} I^*_{N(m)}\rangle = \langle I_{N(n)}\rangle\langle I^*_{N(m)}\rangle$, noting that $\langle I_{N(n)}\rangle$ implies an ensemble average over all $m_{N(n)}(\vec{x})$. This average can be split into two parts: over all configurations where the nth cluster contains $N(n)$ fibres and over the number $N(n)$ itself. Breaking up the average in this way we define $\overline{m}_{\bar{N}}(r) \equiv \langle m_{N(n)}(\vec{x})\rangle$ to be the average mass density of an $\bar{N} \equiv \langle N(n)\rangle$ cluster. Using Eq. (3) and noting that the total average mass in an N cluster is Nw_f, where w_f is defined as the mass per fibre, we can show that

$$\bar{m}_{\bar{N}}(r) = \frac{w_f}{\pi\gamma B^3} R(\bar{N}) f(r/R(\bar{N})). \quad (7)$$

Thus we have $\langle I_{N(n)}\rangle\langle I^*_{N(m)}\rangle = |J_{\bar{N}}(|\vec{k}|)|^2$, where $J_{\bar{N}}(|\vec{k}|)$ is the Fourier transform of $\bar{m}_{\bar{N}}(r)$. To evaluate the exponential term on the right-hand side of Eq. (6) we consider two cases: $n = m$ and $n \neq m$. The first gives unity, while the second depends on the type of effective cluster-cluster interaction between clusters n and m. Defining $\Delta\vec{x}_{n,m} \equiv \vec{x}_n - \vec{x}_m$, we note that the ensemble average over all cluster-network realizations is equivalent to integrating $e^{-2\pi i\Delta\vec{x}_{n,m}}$ over all $\Delta\vec{x}_{n,m}$, weighted by a cluster-cluster pair probability density $g(\Delta\vec{x}_{n,m})$. We also assume, by isotropy, that $g(\Delta\vec{x}_{n,m})$ is independent of the indices n and m, and radially symmetric [16]. The average of the exponential on the right-hand side of Eq. (6) can thus be written as

$$\langle e^{-2\pi i\vec{k}\cdot\vec{\Delta}x_{n,m}}\rangle = \begin{cases} \frac{1}{A}\int_A e^{-2\pi i\vec{k}\cdot\vec{x}} g(|\vec{x}|)\, d\vec{x}, & n \neq m \\ 1, & n = m. \end{cases} \quad (8)$$

Combining the equations above we finally obtain

$$\langle|\hat{M}(\vec{k})|^2\rangle = n_c|J_{\bar{N}}(k)|^2 + \frac{n_c(n_c-1)}{2A}|J_{\bar{N}}(k)|^2\hat{g}(k), \quad (9)$$

where $\hat{g}(k)$ is the Fourier transform of $g(|\vec{x}|)$. Equation (9) comprises two terms. The first represents the spectral density of n_c individual fibre clusters. Substituting this term into Eq. (4) gives the two-point density correlation function of n_c individual $\bar{N}$ clusters. The second term arises due to effective cluster-cluster interactions. The number of clusters n_c can be expressed in terms of a parameter η, defined as the number of fibres per unit area [17]. In particular, we have $n_c = \eta A/\bar{N}$. Writing $\bar{N}$ in terms of the average cluster radius and substituting Eq. (9) into Eq. (4), the following $G_{\bar{N}}(r)$ is finally obtained:

$$G_{\bar{N}}(r) = \frac{4}{\gamma^2 B^3\eta} R^3(\bar{N})\int_0^\infty \Pi^2(k) k J_0(2\pi kr)\, dk + \frac{2}{\gamma^2}\int_0^\infty \Pi^2(k)\hat{g}(k) k J_0(2\pi kr)\, dk, \quad (10)$$

where $\Pi(k)$ (a dimensionless quantity) is given by

$$\Pi(k) = \int_0^\infty f(z) z J_0(2\pi kR(\bar{N})z)\, dz \quad (11)$$

and where J_0 is the Bessel function of order zero. In obtaining Eq. (10) we normalized $G(r)$ by dividing by the square of ηw_f [10,17] and noted that both $\Pi(k)$ and $\hat{g}(k)$ are radially symmetric.

Equation (10) is our main result for the fibre network. The first component in it describes the density-density correlations of a uniformly random distribution [$g(r) = 0$] of fibre clusters. For this case it is easy to show that Eq. (10) becomes $G_{\bar{N}}(r) = R(\bar{N})\Gamma(r/R(\bar{N}))$ where $\Gamma(r)$ is Gaussian for small r and rapidly goes to zero as $r \gg 1$. This dependence on $R(\bar{N})$ in Eq. (10), allows us to extract the typical fibre-cluster size directly from the correlation function.

The second term in Eq. (10) arises due to an effective pair distribution function acting between clusters. This function can lead to nontrivial long-range correlations in the fibre network. Such correlations could arise from hydrodynamics in the sedimentation of particles from suspensions [9]. We have examined a model pair distribution given by $\hat{g}(k) \propto k^{-\chi}$. Figure 4 shows the second term of $G_{\bar{N}}(r)$ for $\chi = 1.1, 1.3$, and 1.6 and $R(\bar{N}) = 3$, where distance is measured in units of B. For $r > R(\bar{N})$ [where the first term of $G_{\bar{N}}(r)$ becomes negligible], we find $G_{\bar{N}}(r) \sim r^{-\alpha}$, where the correlation exponent $\alpha < 1$ decreases continuously as χ is increased from 0 to 2. Since the function $\Pi(k) \approx 0$ for $k > 1/R(\bar{N})$, we expect any effective pair distribution satisfying $g(k) \sim k^{-\chi}$ for small k to give essentially the same power law correlations at large r.

In conclusion, we have presented a model for the statistical properties of disordered 2D fibre networks

formed by deposition processes. The radius of fibre clusters scales with the number of fibres. Similarly, the density profiles of a cluster obey scaling laws, with a universal scaling function for the cases studied here. Starting from the scaling form, we have derived the two-point density-density correlation function for a fibre network due to deposition of clusters, whose spatial distribution is given. In the case of uniform, random deposition of fibre clusters correlations exist over the range of the mean cluster size. However, an effective cluster-cluster interaction can give rise to long-range power law correlations. In this way the final structure of deposited fiber networks may give us information about the effective interactions between fibers in a suspension.

We expect that our $G_{\bar{N}}(r)$ can be compared with experiments on sedimentation of fiberlike particles in suspensions. A prime example of such a process is the formation of laboratory paper sheets, whose final mass density can be measured by the beta-radiogram technique [11]. Our calculations will be compared with long-range correlations observed in such radiogram data in an upcoming publication.

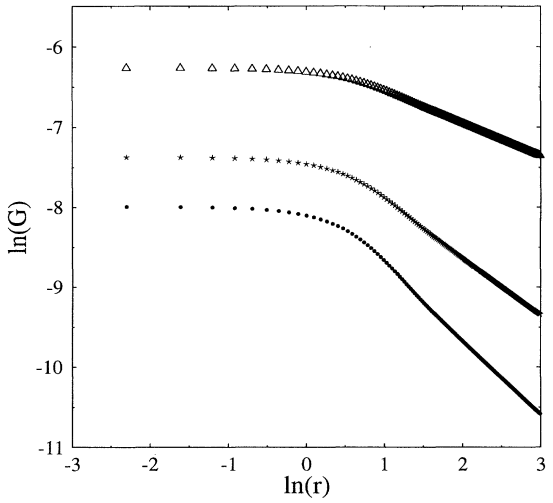

FIG. 4. The correlation function of Eq. (10) with $\hat{g}(k) = k^{-\chi}$, where $\chi = 1.1, 1.3, 1.6$ from bottom to top. In the large r limit power law behavior $r^{-\alpha}$, with $\alpha = 0.92, 0.71, 0.4$, emerges.

This work has been supported in part by the Academy of Finland through the MATRA program.

[1] J. W. Evans, Rev. Mod. Phys. **65**, 1281 (1993).
[2] V. Privman, in *Annual Reviews in Computational Physics,* edited by D. Stauffer (World Scientific, Singapore, 1995), Vol. **3**.
[3] G. Y. Onoda and E. G. Liniger, Phys. Rev. A **33**, 715 (1986); A. Schmit, R. Varoqui, S. Uniyal, J. L. Brash, and C. Pusiner, J. Colloid Interface Sci. **92**, 25 (1983); J. Feder and I. Giaever, J. Colloid Interface Sci. **78**, 144 (1980).
[4] M. Deng and C. T. J. Dodson, *Paper: An Engineered Stochastic Structure* (Tappi Press, Atlanta, GA, 1994).
[5] K. J. Niskanen and M. J. Alava, Phys. Rev. Lett. **73**, 3475 (1994).
[6] P. Nielaba and V. Privman, Phys. Rev. E **51**, 2022 (1995).
[7] N. Ryde, H. Kihira, and E. Matijevic, J. Colloid Interface Sci. **151**, 421 (1992).
[8] C. A. Murray and D. G. Grier, Am. Sci. **83**, 238 (1995).
[9] S. Schwarzer, cond-mat@babbage.sissa.it, no. 9503091.
[10] L. Haugland, B. Norman, and D. Wahren, Svensk Papperstidning no. **10**, 362 (1974).
[11] B. Norman and D. Wahren, Svensk Papperstidning årg. **75**, 807 (1972).
[12] O. J. Kallmes and G. Bernier, Tappi J. **47**, 694 (1964).
[13] R. J. Kerekes and C. J. Schell, J. Pulp Paper Sci. **18**, J32 (1992).
[14] A.-L. Barabási and H. E. Stanley, *Fractal Concepts in Surface Growth* (Cambridge University Press, Cambridge, 1995).
[15] B. Lorenz, I. Orgzal, and H.-O. Heuer, J. Phys. A **26**, 711 (1993).
[16] This assumption is made here only for simplicity, and could be relieved in situations where the cluster-cluster interactions are asymmetric.
[17] This quantity is proportional to mass per unit area, known as the basis weight in paper physics literature, see Ref. [4].